Chapter 13
Dynamic Characterization of Soils Using Various Methods for Seismic Site Response Studies

Pradeep Kumar Dammala and **A. Murali Krishna**

13.1 Introduction

Effective seismic-resistant design of structures requires thorough investigation of underlying soil's response to dynamic loading conditions. Such dynamic behavior of soils is governed by many factors and is represented in terms of strength and stiffness properties [1]. The dynamic soil stiffness is traditionally represented using the strain-dependent properties, often termed as dynamic soil properties: low-strain shear modulus (G_{max}), normalized shear modulus (G/G_{max}), and damping ratio (D) variation with shear strain (γ). The low-strain ($\leq 0.0001\%$) shear modulus (G_{max}) is the maximum dynamic shear stiffness a soil can possess and is linear elastic in nature [2]. With increase in the induced strains, the nonlinearity prevails and plastic strains are induced in the soil grains [3]. This result in the reduction of shear stiffness with shear strains, however in contrast, due to the increased work done, material damping increases [4]. Figure 13.1 illustrates the dynamic soil properties with typical strain ranges and their expected stress–strain response. In addition, the dynamic strength of saturated fine-grained soils is also represented using the ability to resist liquefaction and can be assessed by various field and laboratory equipment [5–8].

The requirement of dynamic soil behavior is application specific for earthquake geotechnical engineering studies. Some studies include liquefaction susceptibility analysis for effective mitigation applications [9]; G_{max} estimation for elastic ground response and fatigue analysis of foundations such as Offshore Wind Turbine (OWT)—[10]; comprehensive dynamic soil properties for Dynamic Soil–Structure Interaction (DSSI) analysis of deep foundations such as piles and caissons [11, 12]

P. K. Dammala · A. Murali Krishna (✉)
Department of Civil Engineering, Indian Institute of Technology Guwahati, Guwahati, India
e-mail: amurali@iitg.ac.in

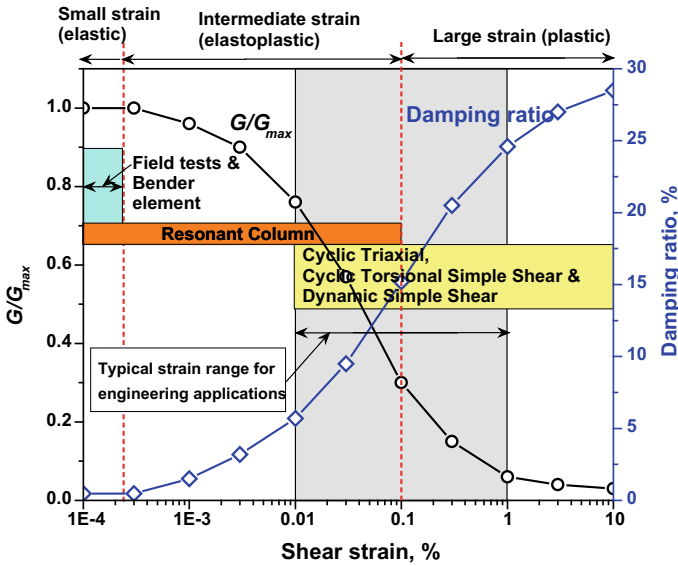P. K. Dammala
e-mail: dammala@iitg.ac.in

Fig. 13.1 Typical representation of strain-dependent dynamic soil properties

and studies involving nonlinear seismic ground response [13, 14]; earth retaining structures [15, 16]; seismic requalification studies [17–19].

Several field and laboratory testing methods have been developed by many researchers to investigate the dynamic behavior of soils [14, 20–24]. Field approaches involve the determination of low-strain properties (shear wave velocity, V_s) while the laboratory techniques yield the required properties over wide strain range. Some of the available field tests include seismic cross/up/down-borehole testing; Multi-channel Analysis of Surface Waves (MASW) [20]. Laboratory testing techniques include Bender element meant for G_{max} determination [22]; Resonant Column (RC) for dynamic soil properties up to a strain range of 0.1% [25]; Dynamic Simple Shear (DSS) for properties from 0.01 to 10% [26]; Cyclic Torsional Simple Shear (CTSS) apparatus for properties at strain range of 0.01–10% [27]; and Cyclic Triaxial (CTX) apparatus over strains >0.01% [28], see Fig. 13.1 for the testing techniques used to obtain the strain-dependent dynamic soil properties. Each testing technique is unique in its application with different advantages and inherent limitations [29].

The present article provides a description of some of the commonly used field and laboratory testing techniques for dynamic characterization of soils. Typical results obtained using the techniques are discussed and appropriate analytical formulations are provided. Furthermore, a seismic ground response study is also presented demonstrating the applicability of the proposed analytical formulations based on the test results.

13.2 Field Tests

Field tests generally involve the measurement of wave velocities propagating through the soil or the response of soil structure systems to dynamic excitation [29]. They can be grouped either into invasive or noninvasive techniques. Invasive methods require at least one borehole while noninvasive techniques (also called surface wave or refraction methods) are based on surface wave measurements. Invasive tests include seismic cross/up/down-borehole survey. Surface wave tests include Spectral or Multichannel Analysis of Surface Waves (SASW or MASW) and seismic refraction tests. This section describes MASW and cross-hole tests in detail with some typical results.

13.2.1 Multichannel Analysis of Surface Waves (MASW)

Multichannel Analysis of Surface Waves (MASW) is a noninvasive seismic survey for evaluating the 1D, 2D, and 3D stiffness profile of the subsurface in terms of shear wave velocity (V_s). This method has been widely used in professional practice due to the speed of implementation and is also budget friendly compared to the other seismic borehole methods. MASW test uses the dispersive characteristics of the surface waves with multi-receiver approach for the stratification of, mostly, the assumed vertically heterogeneous subsurface conditions. Active and passive MASW are different forms which are classified based on the source considered for the generation of surface waves [20]. Figure 13.2 schematically represents the active MASW test setup and instrumentation.

MASW typically consists of three-dependent stages—data acquisition, dispersion analysis, and inversion. Data acquisition is related to acquiring the response of subsurface due to the energy transmitted. Typical active MASW survey requires a sledgehammer as a source of energy, geophones (12 or more) as receivers and data acquisition system for recording and storing the data [30, 31]. Figure 13.3 shows a typical MASW survey with all the steps briefly presented. Upon acquiring the data using geophones at a specific location, data analysis (dispersion and inversion) is performed using computer programs such as SURFSEIS, EasyMASW, and Geopsy. Fixed standards have not been established in the surface wave methods due to the complexities involved in the data interpretation process and the variety of possible approaches to surface wave analysis [32]. However, reliable surface velocity stratification can be achieved by proper parameter selection during the data analysis and recommendations were proposed for efficient filtering techniques [30–32].

Two locations inside the IIT Guwahati campus were considered to provide the subsoil stratification through V_s profile. An array of 24 geophones with 2 m spacing in-between, a 10 kg sledgehammer, and 24-bit data acquisition system were used. Time sampling parameters and data processing using SURFSEIS program can be found in detail in Kashyap et al. [30]. Figure 13.4 presents the final obtained shear wave velocity profile of the chosen locations in the IIT Guwahati campus.
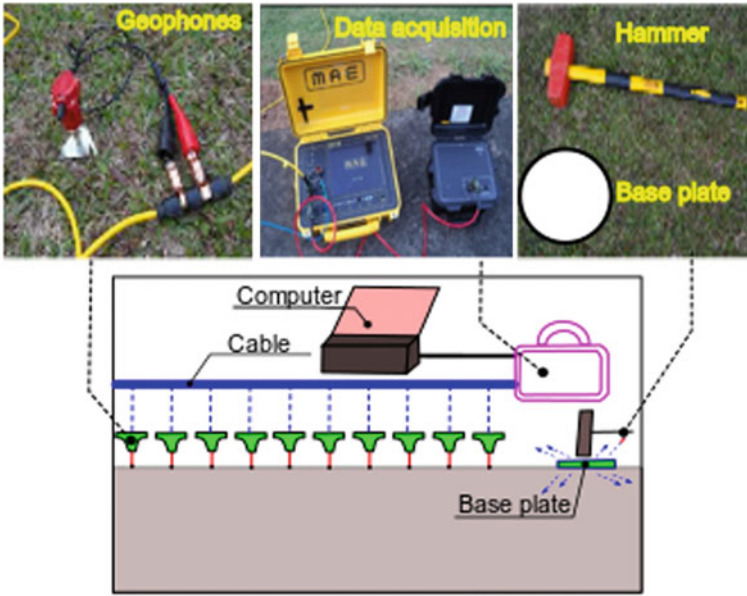
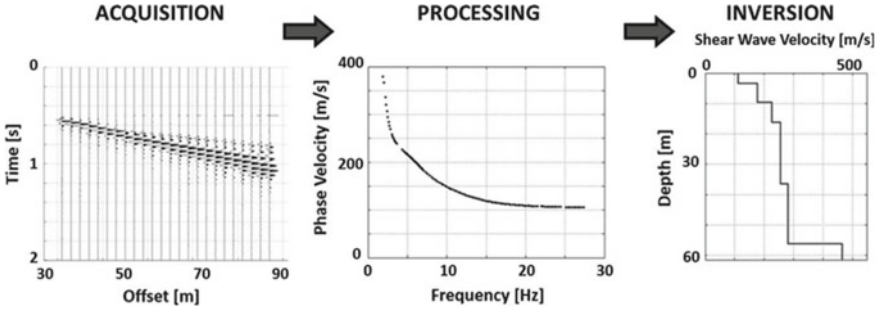**Fig. 13.2** Schematic representation of active MASW setup

Fig. 13.3 Overall procedure of MASW survey [32]

13.2.2 Cross-Hole (CH) Test

Seismic Cross-Hole (CH) survey is an invasive test, whereby the velocity (either P wave or S wave) of the soil deposit is determined using two or more boreholes. The seismic energy is generated at the bottom of a borehole while the sensors in the adjoining borehole at same depth would act as receivers [33]. The mutual distance is measured along with the arrival times of the waves, yielding the velocity profile. Figure 13.5 a shows the essentials of the CH survey. The CH test typically requires two or more boreholes arranged in a straight line array for a better accuracy [29]. Interpretation technique in CH survey is quite straightforward and does not require
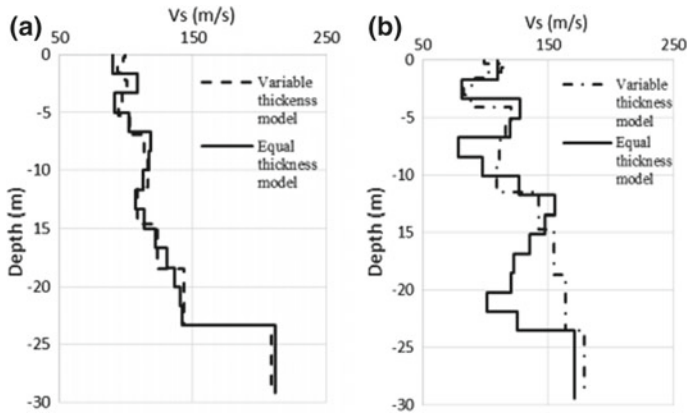
Fig. 13.4 Shear wave velocity variation with depth for the considered soil profiles [30]
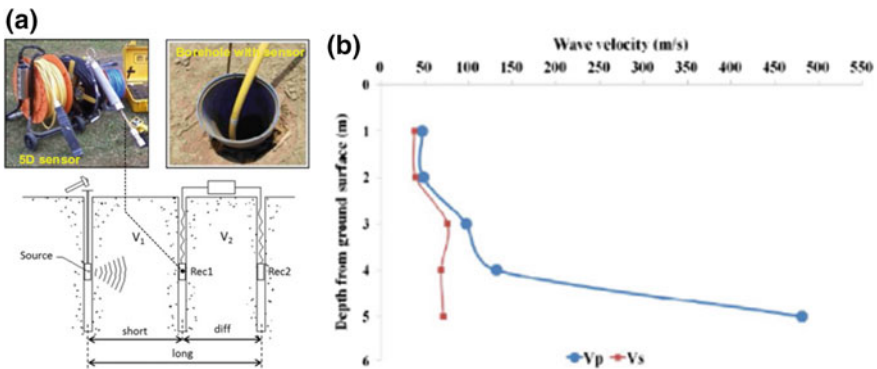

Fig. 13.5 **a** Cross-hole scheme with three boreholes and instrumentation (modified after Garofalo et al. [35]) **b** typical wave profile obtained from CH survey [36]

any complex inversion schemes unlike the surface wave methods and hence the reliability of the results mainly depends on the accuracy of the measurement and in the precision of the instrumentation [34].

Taipodia et al. [36] conducted CH tests at the IIT Guwahati campus to determine the P and S wave velocity profile. The seismic source (a Ballard shear wave generator) is installed in one borehole while the 5D sensor (geophone) is lowered to the same depth as the seismic source in the second borehole. Both the boreholes were 4 m apart and the experiments were conducted by striking the energy generator and recording the signals using the 5D sensor. The P and S wave velocities were determined by picking the "first-arrival time picking" method from the recorded signature [36]. Figure 13.5b presents the P and S wave velocities of the borehole. Further details on arrival time picking and analysis can be found in Taipodia et al. [36].

All the field tests (both invasive and noninvasive) provide the wave velocities with a certain degree of uncertainty like any other geotechnical investigations. The main drawbacks of the field tests are that only low-strain stiffness can be determined and samples for further analysis cannot be arranged. However, one or two field tests are always suggested for projects of relevant importance. The invasive test results for one-dimensional wave profiles are considered relatively reliable compared to the surface wave methods as the uncertainties involved in the testing and data analysis are less. However, the use of borehole surveys is limited in the recent days as they lead to the disturbance in the natural fabric of the soil, ineffective determination of wave velocities in lateral heterogeneity and the requirement of deep borehole for deeper wave velocity determination making it cost ineffective [20, 35].

13.3 Laboratory Element Testing Techniques

Field tests provide dynamic stiffness properties only in the low-strain range and their application is often limited due to the large scale of testing involved. However, laboratory element testing of the collected field samples would provide the desired dynamic properties over a wide strain range. In addition, different field conditions (varying void ratio, plasticity index, confining pressure, etc.) can be explored in the element testing. This section details some of the widely used laboratory element testing techniques to investigate the dynamic soil behavior.
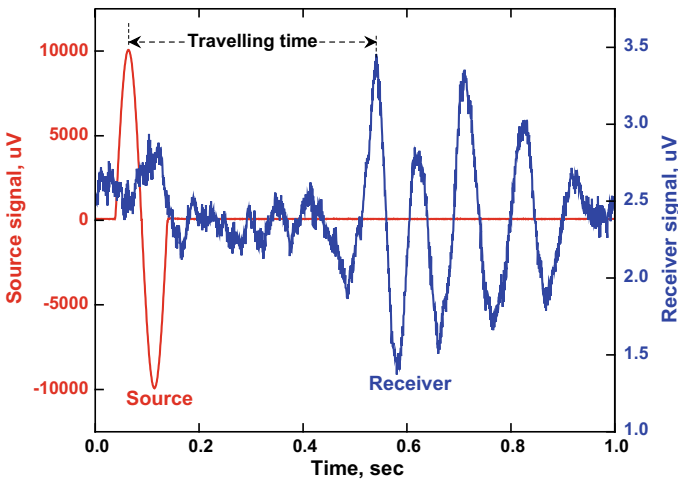
13.3.1 Bender Element Testing

Bender element test is a low-strain test in which the maximum shear modulus (G_{max}) of the soil sample is estimated by transmitting and recording a shear/compressional wave through the sample. Lawrence [37], initially, used the shear plates for measuring the shear wave velocity in sands, and later Shirley and Hampton [38, 39] adopted bender elements for measuring shear wave velocity for marine sediments. Arulnathan et al. [40] recommended methods for effective analysis of bender test results. A bender element is an electro-mechanical transducer which can either bend by change in the induced voltage or generates a voltage as it bends [22]. Two benders are installed on the sample—one at the top plate and the latter at the bottom plate to act as transmitter and receiver, respectively. Figure 13.6 shows a pictorial view of the bender element apparatus, schematic view of the sample conditions and the piezoelectric bender elements used for the testing. These benders can be installed on triaxial, shear, or one-dimensional compressional apparatus and both the tests can be done on the same sample.

A high-frequency electrical pulse (input signal) applied to the transmitter at the bottom platen will deform the bender rapidly resulting in a stress wave, transmitting through the sample toward the receiver. Upon reaching the receiver, the stress wave
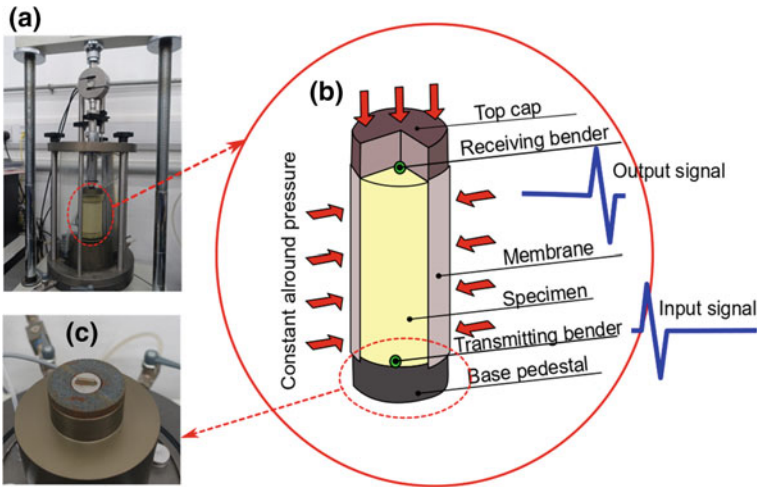
Fig. 13.6 **a** Bender element apparatus **b** schematic view of loading on the sample and **c** view of transmitting bender at the base

Fig. 13.7 Typical input and output signals for a bender element test

generates a voltage pulse which can be measured. Figure 13.7 illustrates the input pulse transmitted and the output signal received at the receiver. The time the stress wave travels through the sample to reach the receiver element is recorded (Fig. 13.7). The velocity (V_s) can be estimated using the effective height of the sample (distance between the two benders at transmitter and receiver—H_s) and the time the stress wave travels (T_s). Using the shear wave velocity and the density of the sample (ρ), maximum shear modulus (G_{max}) can be estimated.

Fig. 13.8 Variation of G_{max} with confining pressure for BP sand at two relative densities
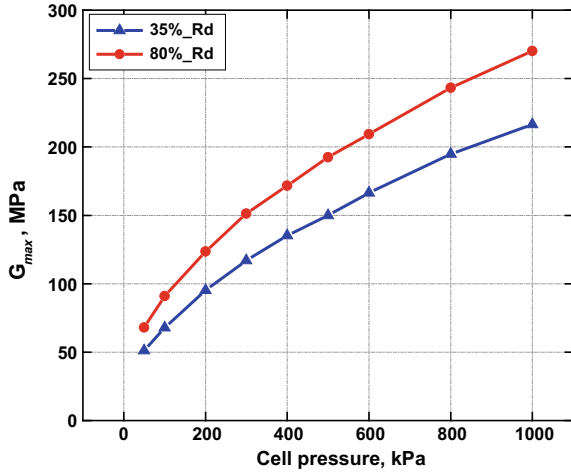
$$G_{\max} = \rho \cdot V_s^2 = \rho \left(\frac{H_s}{T_s} \right)^2 \tag{13.1}$$

Once the velocity is estimated at a particular confining pressure on the sample, the same sample can be used for determining wave velocities at other confining pressures. This is due to the low strains induced in the sample which are not expected to disturb the natural fabric [22]. Figure 13.8 presents the G_{max} results obtained from bender element test on Brahmaputra sand (BP) at two relative densities (R_d) and varying confining pressures. The index and engineering properties of BP sand can be found in the literature [14, 41]. It can be obvious that the increase in the confining pressure and relative density increases the stiffness of the sample.

13.3.2 Resonant Column (RC) Testing

Resonant column (RC) test is used to measure the shear modulus and damping characteristics of soils from low to intermediate strain levels (<0.1%). The basic principle involved in RC testing is the theory of wave propagation in prismatic rods [2], where a cylindrical soil specimen is harmonically excited till it reaches the state of resonance (peak response). The RC technique was initially used for soils by Iida [42], following which the method was further developed by many researchers [43, 44] and was also standardized in ASTM D 4015 [45].

Three different versions of RC apparatus are available, based on the end conditions to constraint the specimen. They are: (a) *Fixed-free* condition [46], in which the bottom end is fixed against rotation while the top end is free to rotate under applied torsion. A known mass is added at the free end to obtain uniform distribution of strain
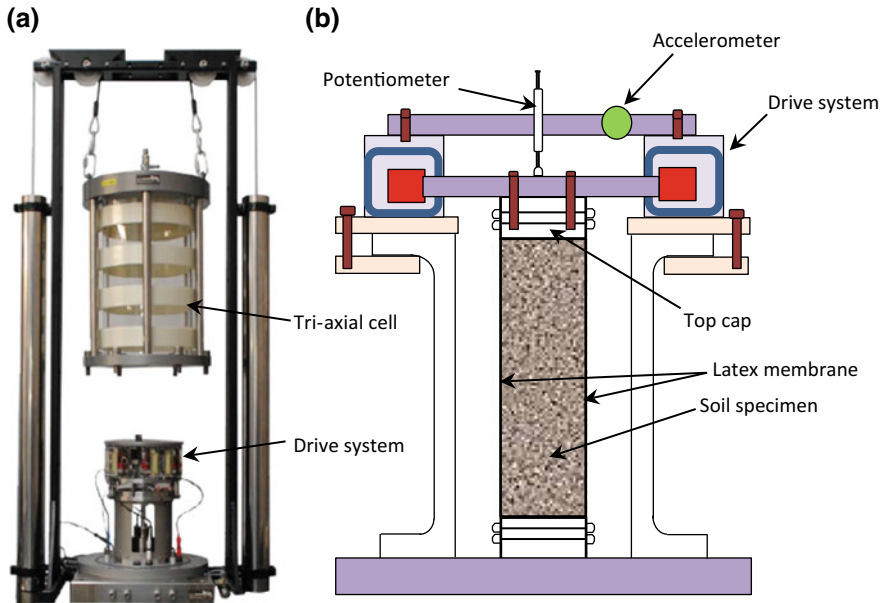
(a) **(b)**

Fig. 13.9 **a** Photographic and **b** schematic view of RC apparatus [14]

throughout the length of the sample, (b) *Spring-base* [47], in which an equivalent spring of stiffness is present at the bottom end of the sample and depending on the stiffness of the spring relative to the stiffness of the soil, the base end condition can be fixed or free, (c) *Fixed-partially restrained* [48], in which the bottom end is fixed while the top cap is partially restrained by springs acting against an inertial mass.

Figure 13.9 shows a fixed-free type of RC apparatus with the instrumentation details. In brief, the soil specimen is excited under a harmonic torsional vibration, induced in the form of electric voltage through the electromagnetic drive system, consisting of four magnets (Fig. 13.9). Initially, a small amount of electric current (say 0.001 V) is passed through the magnetic coils and a broad and fine sweep is conducted to find the exact resonant frequency of the sample [14]. Using this resonant frequency (f_{nz}), height of sample (H), and the instrument constant (β) which can be obtained by calibration of the instrument [45], the shear wave velocity (V_s) and corresponding shear modulus (G) of the sample is determined (Eq. 13.2).

$$G_{\max} = \rho \cdot V_s^2 = \rho \cdot \left(\frac{2\pi f_{nz} H}{\beta} \right)^2 \tag{13.2}$$

Once the resonant frequency is obtained at a particular input voltage, the input current to the coils is switched off to perform a free vibration test. The response of the accelerometer with time is recorded from which the amplitude decay curve is obtained. The peak amplitude of each cycle (A_1—A_{n+1} with n as number of cycles of
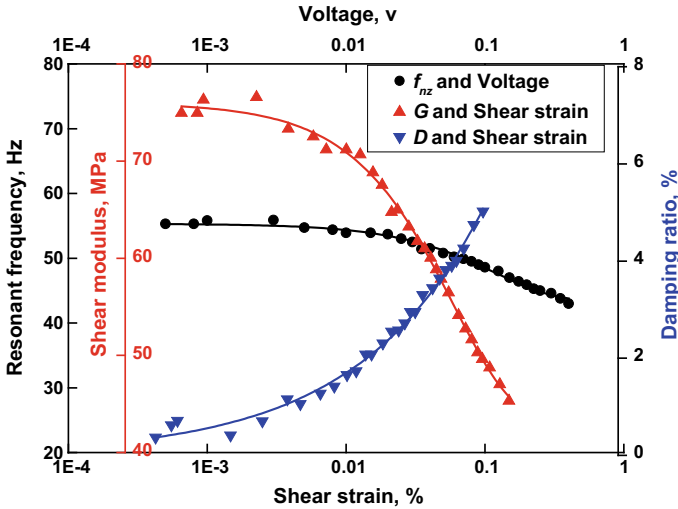
Fig. 13.10 Variation of f_{nz} with input voltage, shear modulus and damping ratio with shear strain for BP sand at 100 kPa effective confining pressure [49]

free vibration) is determined and the corresponding damping ratio (D) is evaluated as suggested by ASTM D 4015 [45].

$$D = \left(\frac{1}{n}\right) \ln\left(\frac{A_1}{A_{n+1}}\right) \tag{13.3}$$

Once the shear modulus and damping ratio at a particular strain (particular voltage) are obtained, then the input voltage to the system is increased to obtain resonant frequency and free vibration response at higher strains. Thus, the voltage is gradually increased at some intervals till the strains reach 0.1% to yield the variation of shear modulus and damping ratio. Figure 13.10 shows the typical variation of resonant frequency with the input voltage, shear modulus, and damping variation with shear strain for BP sand at 30% relative density and 100 kPa effective confining pressure. It can be noted that the increase in the voltage increases the strains induced in the sample resulting in reduced shear stiffness and higher damping ratio [14].

Figures 13.11 presents the variations of shear modulus with shear strain for samples at different confining pressures for BP sand at 30% relative density which were further presented in Fig. 13.12 as modulus ratio along with damping ratio curve. It is obvious that the increase in confining pressure (meaning-overburden depth) increases the stiffness of the sample while damping ratio decreases. Normalized stiffness (ratio of shear modulus to G_{max}) also increases with the confining pressure indicating that the depth of overburden decreases the rate of reduction of the stiffness of sands.
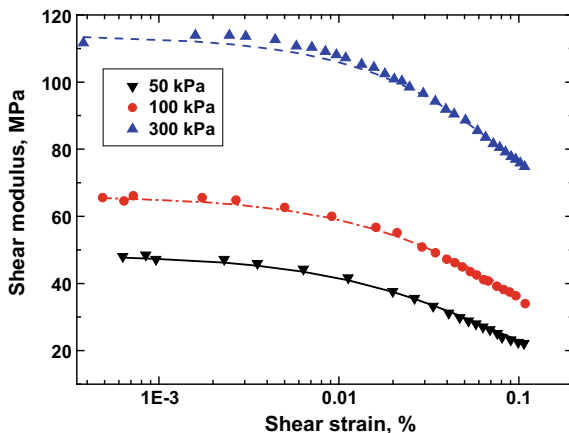
Fig. 13.11 Variation of shear modulus with shear strain for BP sand at different confining pressures for 30% relative density [14]
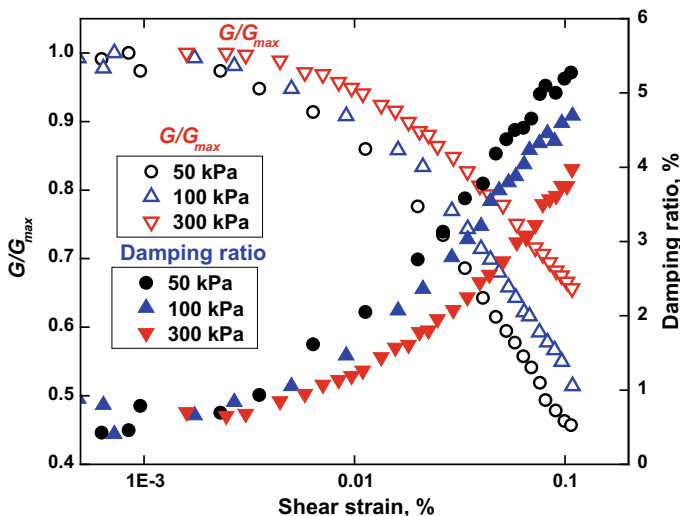
Fig. 13.12 Variation of modulus ratio and damping ratio with shear strain for BP sand at different confining pressures for 30% relative density [14]

13.3.3   Cyclic Triaxial (CTX) Testing

Cyclic Triaxial (CTX) test is a high strain test, which can be used for determining both the dynamic soil properties and liquefaction potential of soils [6, 41]. The strain range typically tested in this apparatus is 0.01–10%. Seed and Lee [6], initially, used CTX apparatus for assessing liquefaction potential of saturated sands while

many researchers [28, 41, 50] adopted the apparatus for determining high-strain dynamic soil properties. Kumar et al. [51] utilized CTX apparatus for determining the dynamic behavior of northeast Indian cohesive soil and also for assessing its liquefaction potential. Lombardi et al. [52] used CTX apparatus to investigate the post-liquefaction behavior of silica sands for application in pile foundations subjected to liquefaction-induced stresses. Both the dry and saturated samples can be tested using the apparatus [53]. Irregular dynamic excitations can also be applied to investigate the effect of realistic earthquake motions [41]. The apparatus can be used for both the stress- and strain-controlled testing [54, 55].

In the CTX apparatus, the soil sample is enclosed inside a triaxial cell through which harmonic axial loads using the servo-controlled actuator at the top can be applied and necessary instrumentation is installed to measure the deformations (axial) and pressures (cell pressure and pore pressure). Figure 13.13 shows a picture of typical CTX setup and various parts associated with it. The details about sample preparation, CTX setup, and testing methodology can be found in the literature [24, 41]. Figure 13.14 presents the typical results of liquefaction potential of BP sand using the CTX system. The stress-controlled test results are presented in Fig. 13.14, which shows a cyclically varying deviatoric stress of ± 20 kPa on the sample applied at 1 Hz frequency (Fig. 13.14a). Liquefaction susceptibility of a soil sample can be represented using the pore water pressure ratio (r_u) which is the ratio of excess pore pressures (Δu) to the mean effective confining pressure (σ'_c). Figure 13.14b shows the variation of axial strain and r_u with loading cycles. It can be noted that the sudden increase of axial strain was attributed to the full liquefaction condition. Also, the stress–strain response of the BP sand is presented in terms of deviatoric stress and axial strain (Fig. 13.14c) and also shear stress and shear strain (Fig. 13.14d). The possible limitation in the CTX apparatus is that the shear strains have to be estimated from the axial strains by assuming a Poisson's ratio, unlike the DSS apparatus, whereby the shear displacements can directly be applied to the specimens.

Figure 13.15 presents the variation of average pore water pressure ratio with loading cycles for BP sand at 30% relative density. The results are related to the strain-controlled tests performed at 100 kPa effective confining pressure. An increase in the pore pressure ratio can be observed with increase in the input strains and the BP sand did not show complete liquefaction for low strains (<0.075%) even up to 40 cycles of loading. However, with the strains beyond 0.075%, increased the tendency toward liquefaction has been noticed with the input strains. Liquefaction was even observed below five loading cycles for high strains (0.75%) which shows that high-intensity ground motions would lead to rapid liquefaction in the sandy deposits [41].

13.3.4 Dynamic Simple Shear (DSS) Testing

Dynamic Simple Shear (DSS) apparatus can be used to investigate the dynamic behavior of soils from intermediate (0.01%) to high strains (up to 10%). Simple Shear device dates back almost half a decade (1950s). The device was initially developed
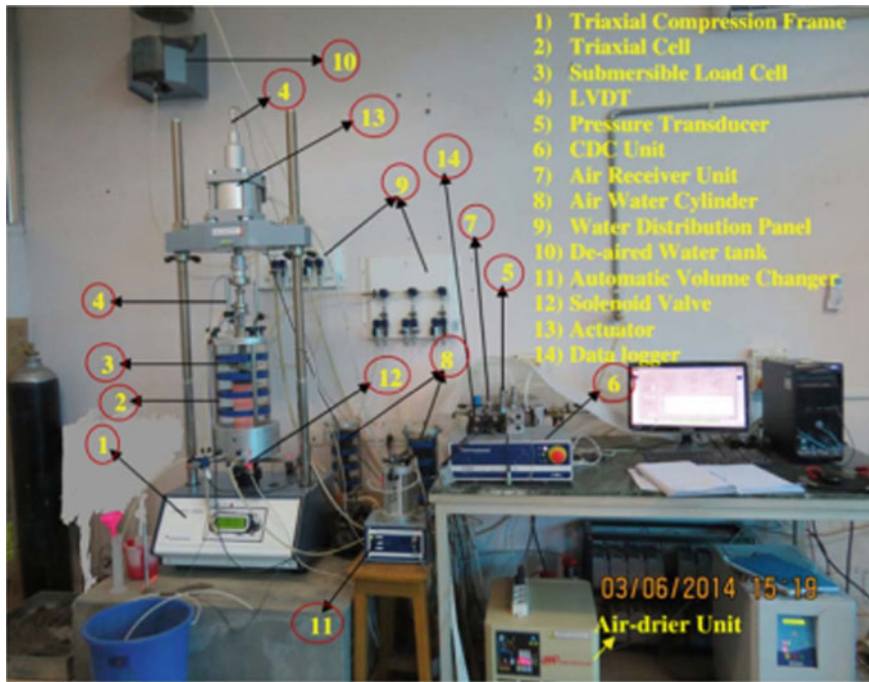
Fig. 13.13 Cyclic triaxial setup and components [41]

in the UK by Roscoe [56], Scandinavia at SGI [57], and at NGI [26]. Later, Peacock and Seed [58] extended the simple shear to assess the liquefaction potential and cyclic strength of soils and named as Dynamic Simple Shear (DSS). A pictorial view of the apparatus and a schematic view of the soil sample during loading are shown in Fig. 13.16. The device is similar to a simple shear except that the provision for cyclic loading through servo-controlled actuator. Axial and lateral displacements during the testing can be monitored using the LVDTs attached over the sample. The main advantage of DSS over the triaxial apparatus is that a shear stress/strain can be directly simulated with the two-way controlled shearing [59]. The soil specimen is contained using laminated circular rings and during shearing, the rings follow the movement of soil specimen, see Fig. 13.16 for details. The confinement is provided through the constant axial stress.

Typical results obtained from the DSS apparatus are presented briefly in this section. Figure 13.17 presents the cyclic stress–strain response (also called hysteresis loops) of BP sand prepared at a medium relative density at normal stress of 100 kPa. The cyclic shear loads were applied for 1000 cycles (N), however, Fig. 13.16 shows only the first 10 cycles for brevity. Using the hysteresis loops, one can calculate the strain-dependent dynamic shear stiffness and damping ratio [41, 59]. An important aspect of hysteresis loops needs to be noted: at high shear strain or larger loading cycles, an asymmetricity in the shape of the loop is observed [41], please see
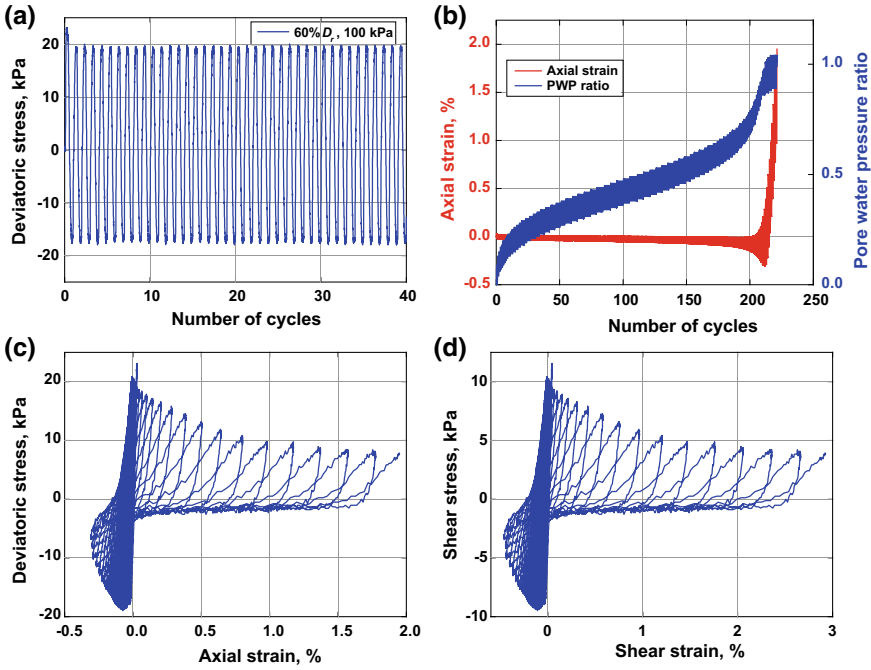
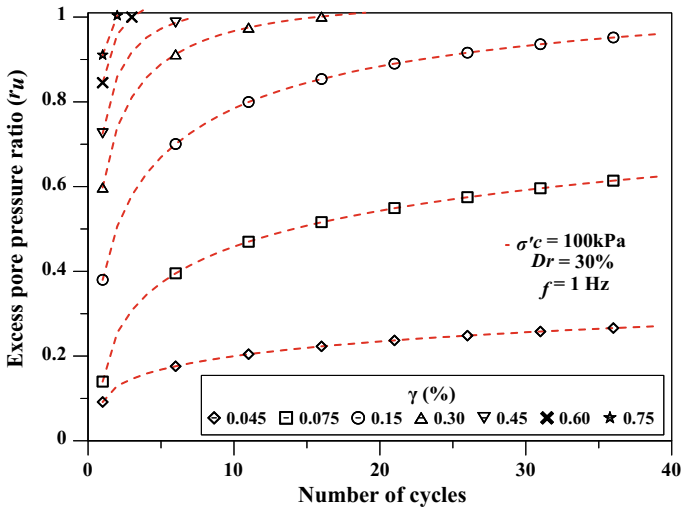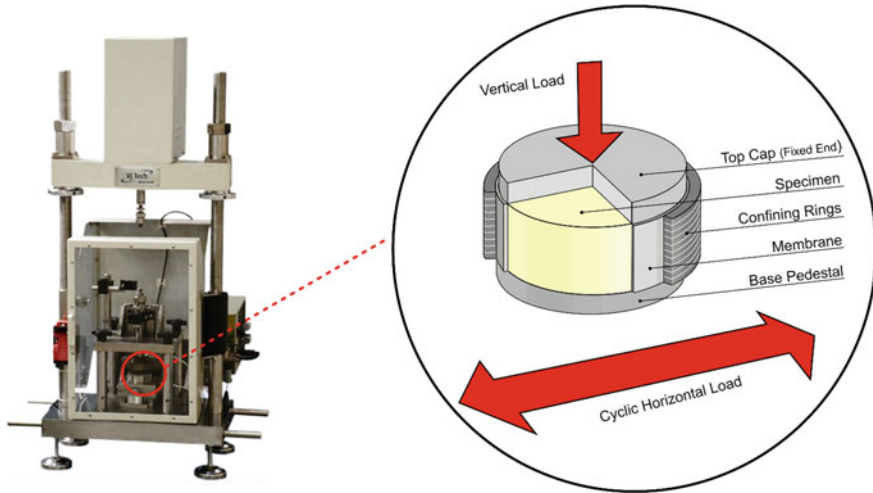**Fig. 13.14** Typical results of CTX apparatus for liquefaction assessment on BP sand

Fig. 13.15 Variation of pore water pressure ratio for BP sand at 100 kPa effective confining pressure [49]

Fig. 13.16 Pictorial and schematic of DSS apparatus

Fig. 13.17 Hysteresis loops for BP sand at three confining pressures for medium density sample
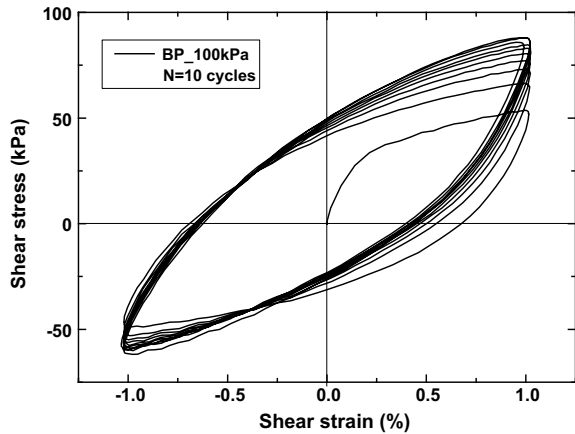

Fig. 13.17 for details. As the dynamic soil behavior is strain dependent, the dynamic soil properties should also be based on the realistic asymmetric loops rather than the traditional symmetric loop calculations. In this view, Kumar et al. [41] presented a method to calculate the strain-dependent properties using the realistic asymmetric loop. Figure 13.18 describes the methodology followed and the corresponding formulations.

Figure 13.19 presents the variation of shear modulus and damping ratio of BP sand evaluated using the asymmetric loop formulations proposed by Kumar et al. [41]. Reduction in shear modulus with shear strains is obvious with increase in shear strain, however, an untraditional trend of increase and decrease of damping ratio with
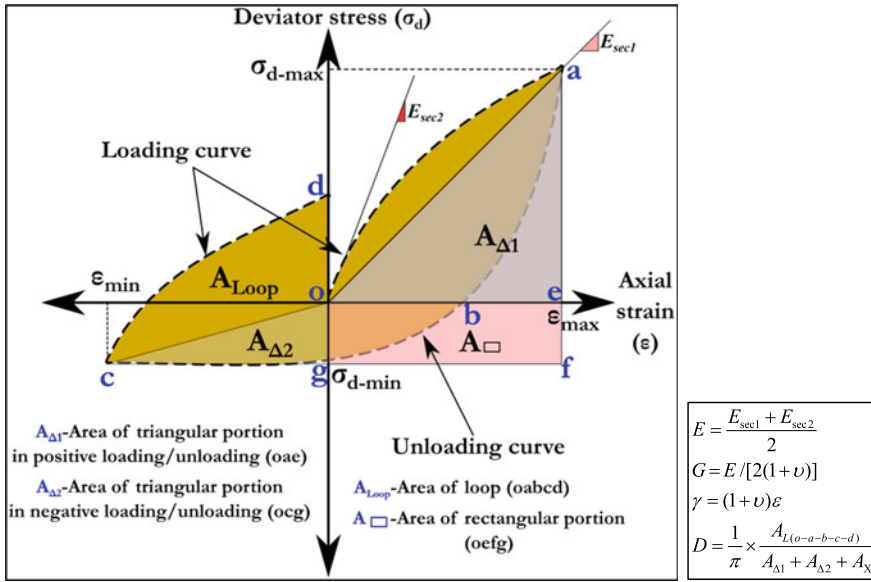
Fig. 13.18 A typical asymmetric loop with formulations for dynamic soil properties determination (modified after Kumar et al. [41])
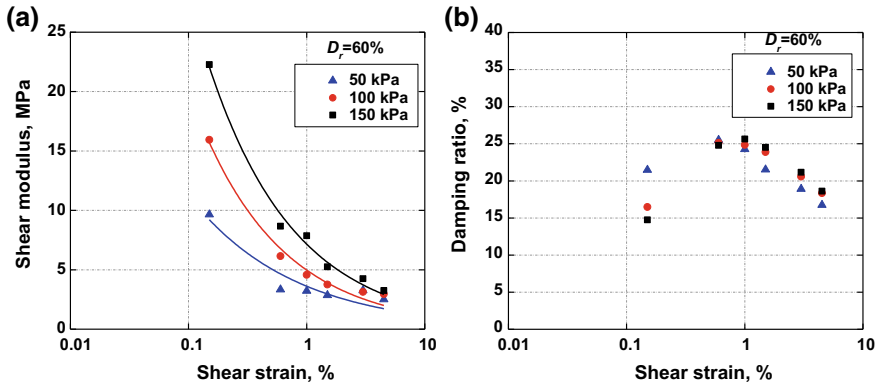
Fig. 13.19 Variation of shear modulus and D with shear strain for BP sand at 60% relative density [49]

shear strain has been observed. This uncommon damping behavior is attributed to the realistic asymmetric loops considered for the evaluation [41].

Once the dynamic soil properties at different shear strains are determined using independent apparatus, the data needs to be combined for a comprehensive data over wide strain range. Figures 13.20 and 13.21 provide the data determined using RC and DSS for BP sand at different relative densities and confining pressures, respectively. Also, the literature suggested [60, 61] ranges of modulus and damping

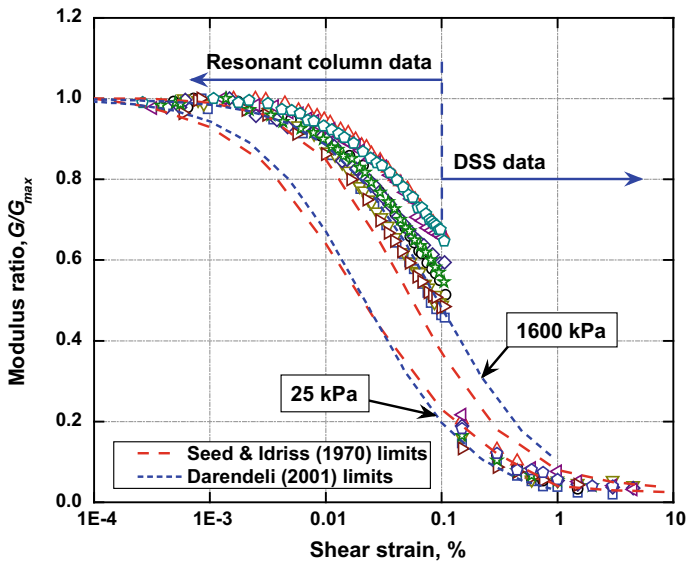**Fig. 13.20**   Modulus ratio variation for BP sand determined from RC and DSS testing

curves for sands are presented (Figs. 13.20 and 13.21). It can be observed that the modulus values fall rightwards in the low-strain range than the Seed and Idriss [60] suggested ranges and follow the suggested range in the high strain levels. Similarly, damping ratio values fall below the suggested ranges, meaning-damping ratio would be overestimated if the site-specific data is not utilized for earthquake geotechnical applications [14, 62].

13.4   Analytical Comparisons

Analytical formulations are required in cases where laboratory data is insufficient for the required conditions. This section describes the analytical comparisons fitted to the laboratory data of dynamic soil properties to the literature suggested formulations.

13.4.1 G_{max}

Several forms of G_{max} estimation are available in the literature [63]. Out of the existing G_{max} formulations, the equation (Eq. 13.4) proposed by Hardin [64] is being considered most often in the earthquake geotechnical applications [63, 65, 66] due to its dimensional consistency and application even to soils of large void ratio [21].
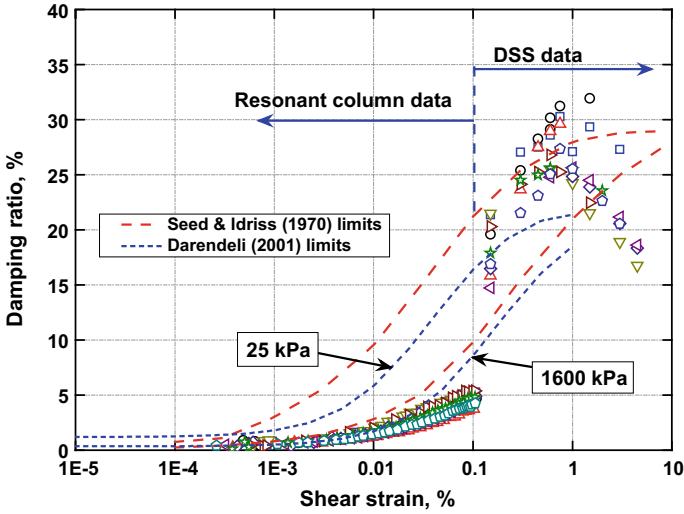
Fig. 13.21 Modulus ratio variation for BP sand determined from RC and DSS testing

Fig. 13.22 Fitted G_{max} results in Eq. 13.4
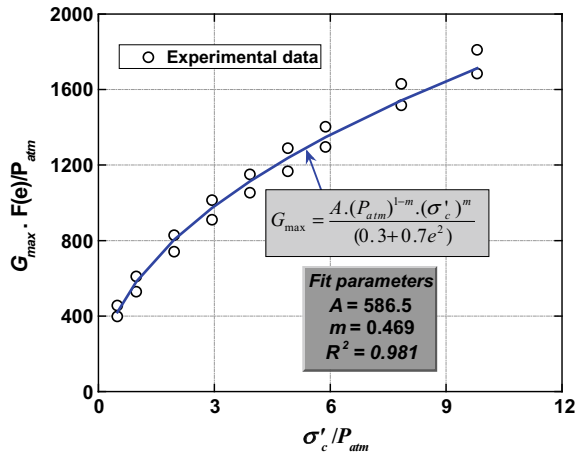
$$G_{\max} = \frac{A \times (P_a)^{1-m} \times (\sigma'_c)^m}{(0.3 + 0.7e^2)} \qquad (13.4)$$

where P_a is atmospheric pressure (101 kPa), A is a constant depending on the type of soil, and m is a stress-dependent factor. The bender element tests performed on BP sand were considered for the regression analysis to obtain the best-fit parameters based on the equation (Eq. 13.4). Figure 13.22 shows the regression analysis of the bender data and the obtained best-fit parameters—$A = 586.5$, $m = 0.469$ with a correlation coefficient of $R^2 = 0.981$.

Fig. 13.23 Variation of normalized modulus to the normalized shear strain for BP sand

13.4.2   G/G$_{max}$ *and Damping*

Similarly, analytical formulations are required for modulus reduction and damping ratio variation with shear strain. Hyperbolic and modified hyperbolic stress-de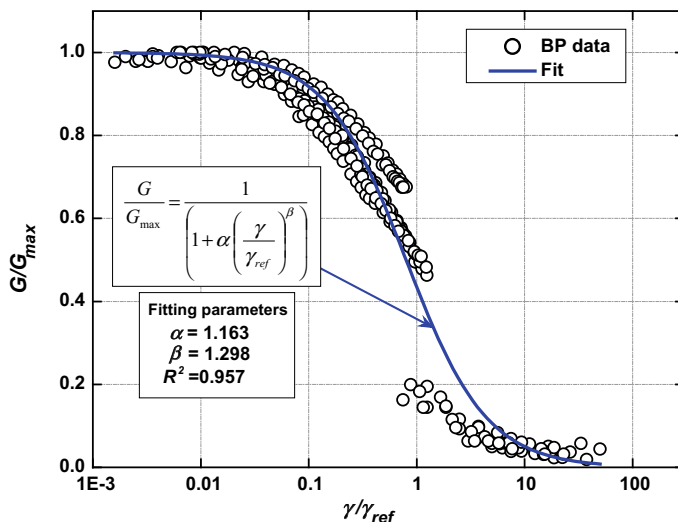pendent equations were proposed by various researchers in order to model both the modulus degradation and damping variation [60, 61, 67–71]. Matasovic and Vucetic [71] formulation (Eq. 13.5) was found to be satisfactorily simulating the modulus degradation behavior.

$$\frac{G}{G_{max}} = \frac{1}{1 + \beta \left(\frac{\gamma}{\gamma_{ref}}\right)^{\alpha}} \tag{13.5}$$

where γ_{ref} is the reference shear strain (shear strain at G/G_{max} value of 0.5 according to Darendeli [61] and α and β are the curve-fitting parameters adjusting the shape of the modulus curve. As the shape of modulus curve is soil specific and hence, the corresponding α and β needs to be determined from the regression analysis of experimental data. Figure 13.23 presents the regression analysis results in terms of variation of normalized modulus to the normalized shear strain for BP sand. The obtained best-fit parameters are also mentioned—$\alpha = 1.163$ and $\beta = 1.298$ with a correlation coefficient of 0.957. Similar simplified regression analysis has been performed by Dammala et al. [14].
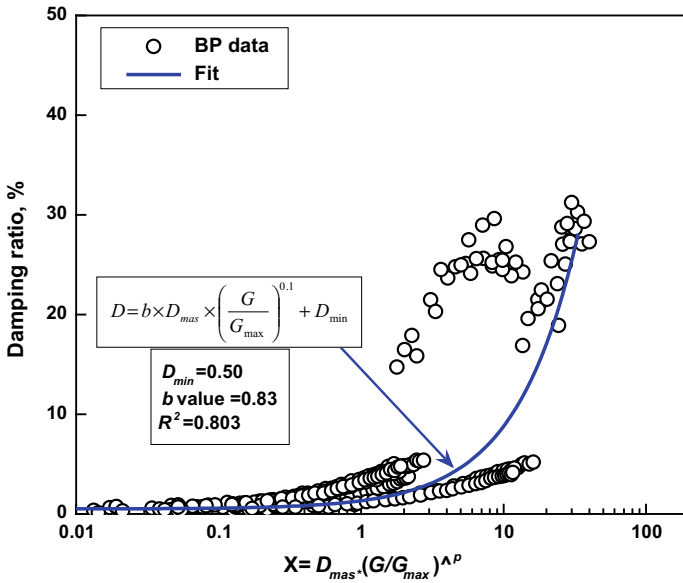
Fig. 13.24 Damping ratio variation with masing damping combined with modulus ratio

Similar to the modulus reduction, analytical expressions for evaluating damping ratio at a given shear strain was also proposed by several researchers [61, 67–69]. Darendeli [61] related damping ratio (Eq. 13.6) with the modulus reduction and achieved reasonable estimates.

$$D(\%) = b \times D_{mas} \times \left(\frac{G}{G_{max}} \right)^p + D_{min} \tag{13.6}$$

where b and p are the scaling coefficients adjusting the high-strain damping ratio (p considered as 0.1), D_{mas} is the masing damping (function of shear strain and the curvature coefficient (α)), and D_{min} is the minimum damping ratio at the lowest possible shear strain (0.5% based on the experimental results). A regression model is run to find the best fit values of b. A b value of 0.83 is found with an R^2 of 0.803. Figure 13.24 presents the simplified regression analysis for damping ratio.

The final stiffness curves (both modulus and damping) of BP sand can be estimated using the regression coefficients (α, β, and b) at any required σ'_c [14]. Such stiffness curves can act as a ready-made tool for design engineers, especially during the design of important structures or the seismic requalification works in the northeastern Indian region.

Fig. 13.25 Pore water
pressure ratio variation of BP
sand [49]
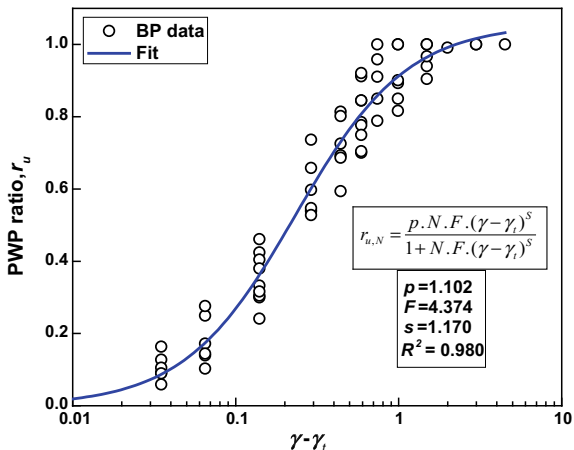
13.4.3 Liquefaction Potential

Liquefaction resistance or susceptibility of soils can be modeled reliably using the pore water pressure (PWP) formulations. The PWP models simulate the generation and dissipation of excess pore pressures during cyclic loading. Numerous PWP models, ranging from simple to complex nature, are available in the literature, see for example—Hashash et al. [72], Dobry et al. [73], Martin et al. [74], Byrne et al. [75]. However, to perform nonlinear effective stress analysis, some commercial programs such as DEEPSOIL [76], employ extended Dobry et al. [73] PWP model as the required input parameters can be efficiently obtained by performing stress/strain-controlled CTX/DSS tests on saturated soil samples. Based on the strain-controlled CTX tests on sandy soil, Vucetic and Dobry [77] extended the basic PWP model developed by Dobry et al. [73] (Eq. 13.7). The model emphasizes the generation of PWP with the number of cycles (N) and applied cyclic shear strain.

$$r_{u,N} = \frac{p \cdot N \cdot F \cdot (\gamma - \gamma_t)^S}{1 + N \cdot F \cdot (\gamma - \gamma_t)^S} \tag{13.7}$$

where $r_{u,N}$ = excess PWP ratio at N number of cycles; γ = cyclic shear strain amplitude; p, F, and s are the curve-fitting parameters; and γ_t is the threshold shear strain below which no significant PWP is generated and is considered as 0.01% [3]. The fitting parameters (p, F, and s) are obtained by best fitting of the pore pressure model on the obtained experimental data of BP sand. Figure 13.25 depicts the obtained results of the PWP model with the fitting parameters. Since the dynamic properties (shear modulus and damping ratio) of BP were evaluated for the first cycle ($N = 1$), the fitting parameters of the PWP model have also been evaluated for the first loading cycle ($N = 1$).
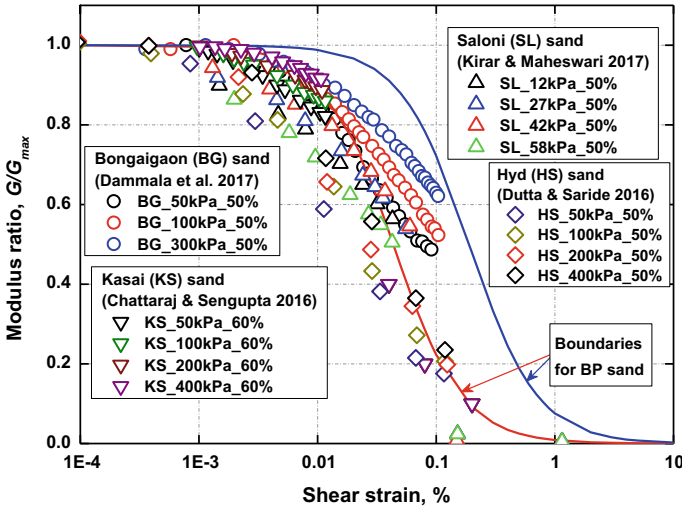
Fig. 13.26 Modulus ratio of Indian sandy soils

13.5 Indian Soil Data

Modulus and damping ratio of Indian sandy soils has been collected from the literature and is shown in Figs. 13.26 and 13.27, respectively, along with the boundaries proposed for BP sand. Data of four sandy soils determined by various laboratory element tests was presented—Bongaigaon sand from northeast India [14], Kasai sand of eastern India (Kolkata) [65], Saloni sand of northern India [78, 79], and sandy soil from southern India (Hyderabad region) [80]. Though the proposed modulus and damping boundaries for BP sand are close to the other sands data, however, there is still some gap exists in both the damping and modulus.

13.6 Application of Established Soil Properties

A one-dimensional nonlinear (NL) time-domain effective stress GRA, incorporating the PWP generation and dissipation, has been performed to demonstrate the applicability of proposed dynamic soil properties and liquefaction parameters. The computer program *DEEPSOIL* [76] has been used for the analysis as it is a widely used nonlinear time-domain site response analysis program which utilizes a discretized multi-degree-of-freedom lumped parameter model of the 1D soil column. The hysteretic soil response is captured by a pressure-dependent hyperbolic model that represents the backbone curve of the soil along with the modified extended unload–reload Masing rules [72, 81]. Further details about the theoretical back-
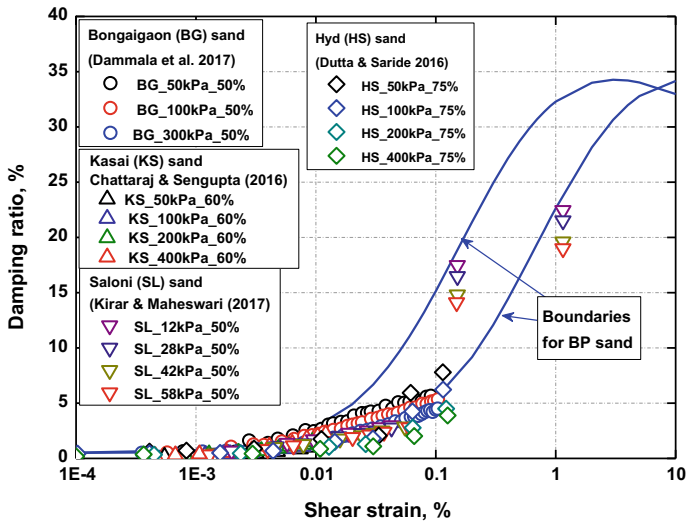
Fig. 13.27 Damping ratio of Indian sandy soils

ground of the methodology can be found in [76, 82]. Similar GRA studies for typical sites in Guwahati city were conducted by [14, 83, 84].

Soil profile considered for the present study is located near the shore of Brahmaputra river in Guwahati, which is considered as one of the most active seismic regions of the country with 0.36 g as the expected Peak Bed Rock Acceleration (PBRA) [85]. Figure 13.28 presents the location of the soil profile considered and the seismicity of the region. Dammala et al. [14, 19] details the soil stratigraphy and further details regarding the parameters considered for the analysis. In the wake of prior warnings issued by the seismologists that this region is prone to a pounding seismic event in the near future, several requalification studies were conducted in this region [19, 86]. Four recorded ground motions of varying ground motion parameters have been used for the analysis (Table 13.1).

Figure 13.29 presents the ground response analysis results in terms variation of Peak Ground Acceleration (PGA), peak shear strain, and PWP ratio along the depth of the profile. Amplification for low-intensity ground motions was observed while deamplification/attenuation for high-intensity motions was noticed. This pattern of amplification/attenuation can be justified through the damping characteristics of the soil sediments, whereby the surficial stratum which is loose is expected to experience high shear strains (Fig. 13.29b) leading to high damping, thereby resulting in attenuation of the incoming waves. In contrast, the low-intensity motions induce less strain for which the damping is also low leading to high amplifications [88, 89]. In addition, the ground motions with PBRA > 0.10g liquefy the surficial stratum which is also justified through the results obtained using the semi-empirical approach proposed by Idriss and Boulanger [7].
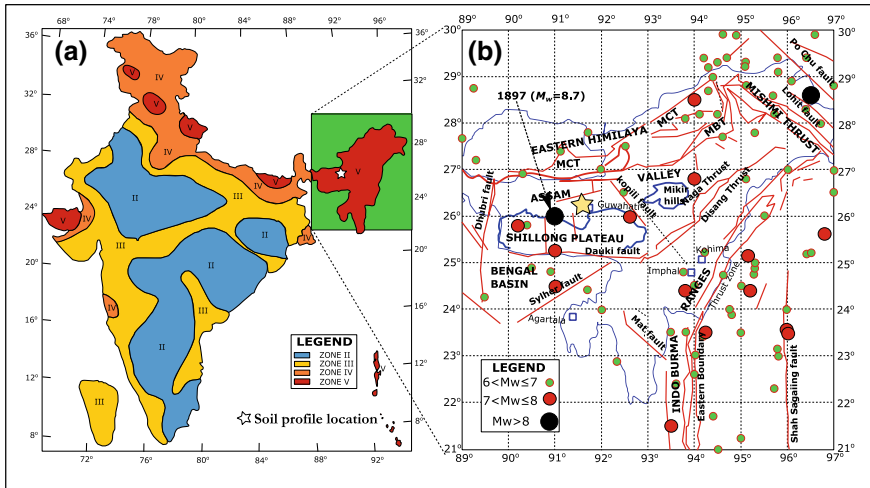
Fig. 13.28 **a** Seismic zonation map of India [85] **b** seismotectonic faults in the northeastern India [87]

Table 13.1 Strong motion parameters of the considered ground motions (modified from Dammala et al. [49])

Earthquake parameters	Sikkim 2011 earthquake	Sonitpur 2009 earthquake	Indo-Burma 1988 earthquake	Indo-Burma 1988 earthquake
Short name	SKM 0.02g	SONIT 0.03g	INDBUR 0.18g	INDBUR 0.33g
Date of occurrence	18-09-2011	19-08-2009	06-08-1988	06-08-1988
Moment magnitude	6.8	4.9	7.2	7.2
Epicenter	27.52° N 88.04° E	26.60° N 92.50° E	25.15° N 95.13° E	25.15° N 95.13° E
Recording station	IIT Guwahati	Guwahati	Diphu	Diphu
Distance from source (km)	378	424	193	193
PBRA (g)	0.02	0.031	0.18	0.330
Depth (km)	20	20	91	91

13.7 Summary and Concluding Remarks

Determining the dynamic behavior of soil is a prerequisite for an efficient earthquake-resistant foundation design. Dynamic behavior of soil can be represented using low-strain shear modulus, modulus, and damping variation with shear strain along with the liquefaction potential. Several laboratory and field techniques are available and this article describes some of the widely used field and laboratory tests for assessing
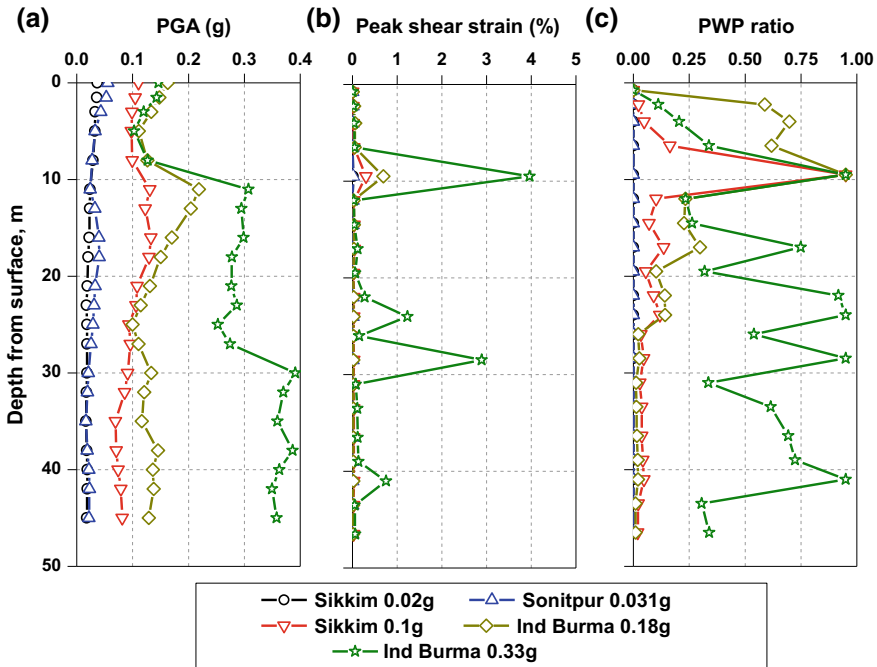
Fig. 13.29 Profiles of **a** PGA **b** peak shear strain and **c** PWP ratio [49]

the dynamic behavior of soils. Typical results using each test are also presented for a comprehensive understanding of the reader. As the field test can only provide the low-strain dynamic stiffness characteristics, it is therefore, necessary to perform laboratory element tests to completely understand the dynamic behavior of soils over wide strain range. Analytical formulations were proposed based on the laboratory test results and the data is compared to the data collected from literature for Indian sandy soils. Finally, a seismic ground response study has been conducted to demonstrate the applicability of proposed formulations.

References

1. Kumar, S.S., Murali Krishna, A., Dey, A.: Parameters influencing dynamic soil properties: a review treatise. Int. J. Innov. Res. Sci. **3**, 47–60 (2014)
2. Hardin, B.O., Richart, F.E.: Elastic wave velocities in granular soils. J. Soil Mech. Found. Div. **89**, 33–65 (1963)
3. Vucetic, M.: Cyclic threshold shear strains in soils. J. Geotech. Geoenviron. Eng. **120**, 2208–2228 (1995)
4. Kramer, S.L.: Geotechnical Earthquake Engineering, 1st edn. Prentice-Hall, New Jersey (1996)
5. Seed, H.B., Idriss, I.M.: Simplified procedure for evaluating soil liquefaction potential. J. Soil Mech. Found. Div. **97**, 1249–1273 (1971)

6. Seed, H.B., Lee, K.L.: Liquefaction of saturated sands during cyclic loading. J. Soil Mech. Found. Div. **92**, 105–134 (1966)

7. Idriss, I.M., Boulanger, R.W.: Semi-empirical procedures for evaluating liquefaction potential during earthquakes. Soil Dyn. Earthq. Eng. **26**, 115–130 (2006). https://doi.org/10.1016/j.soildyn.2004.11.023

8. Andrus, R., Stokoe, K.H.: Liquefaction resistance of soils from shearwave velocity. J. Geotech. Geoenviron. Eng. ASCE **126**, 1015–1025 (2000)

9. Krishna, A.M., Madhav, M.R.: Engineering of ground for liquefaction mitigation using granular columnar inclusions: recent developments. Am. J. Eng. Appl. Sci. **2**, 526–536 (2009). https://doi.org/10.3844/ajeassp.2009.526.536

10. Arany, L., Bhattacharya, S., Macdonald, J.H.G., Hogan, S.J.: Closed form solution of Eigen frequency of monopile supported offshore wind turbines in deeper waters incorporating stiffness of substructure and SSI. Soil Dyn. Earthq. Eng. **83**, 18–32 (2016). https://doi.org/10.1016/j.soildyn.2015.12.011

11. Wu, G., Finn, W.D.L.: Dynamic nonlinear analysis of pile foundations using finite element method in the time domain. **3**, 44–52 (1997)

12. Mondal, G., Prashant, A., Jain, S.K.: Simplified seismic analysis of soil-well-pier system for bridges. Soil Dyn. Earthq. Eng. **32**, 42–55 (2012). https://doi.org/10.1016/j.soildyn.2011.08.002

13. Phillips, C., Hashash, Y.M.A.: Damping formulation for nonlinear 1D site response analyses. Soil Dyn. Earthq. Eng. **29**, 1143–1158 (2009). https://doi.org/10.1016/j.soildyn.2009.01.004

14. Dammala, P.K., Krishna, A.M., Bhattacharya, S., et al.: Dynamic soil properties for seismic ground response studies in Northeastern India. Soil Dyn. Earthq. Eng. **100**, 357–370 (2017). https://doi.org/10.1016/j.soildyn.2017.06.003

15. Pain, A., Choudhury, D., Bhattacharyya, S.K.: Effect of dynamic soil properties and frequency content of harmonic excitation on the internal stability of reinforced soil retaining structure. Geotext. Geomembr. **45**, 471–486 (2017). https://doi.org/10.1016/j.geotexmem.2017.07.003

16. Krishna, A., Bhattacharjee, A.: Behavior of rigid-faced reinforced soil-retaining walls subjected to different earthquake ground motions. Int. J. Geomech. **17**, 6016007 (2017). https://doi.org/10.1061/(ASCE)GM.1943-5622.0000668

17. Dash, S.R., Govindaraju, L., Bhattacharya, S.: A case study of damages of the Kandla Port and Customs Office tower supported on a mat-pile foundation in liquefied soils under the 2001 Bhuj earthquake. Soil Dyn. Earthq. Eng. **29**, 333–346 (2009). https://doi.org/10.1016/j.soildyn.2008.03.004

18. Sarkar, R., Bhattacharya, S., Maheshwari, B.K.: Seismic requalification of pile foundations in liquefiable soils. **44**, 183–195 (2014). https://doi.org/10.1007/s40098-014-0112-8

19. Dammala, P.K., Bhattacharya, S., Krishna, A.M., et al.: Scenario based seismic re-qualification of caisson supported major bridges? A case study of Saraighat Bridge. Soil Dyn. Earthq. Eng. **100**, 270–275 (2017). https://doi.org/10.1016/j.soildyn.2017.06.005

20. Park, C.B., Miller, R.D., Xia, J.: Multichannel analysis of surface waves. Geophysics **64**, 800–808 (1999). https://doi.org/10.1190/1.1444590

21. Chung, R., Yokel, F., Drnevich, V.: Evaluation of dynamic properties of sands by resonant column testing. Geotech. Test. J. **7**, 60 (1984). https://doi.org/10.1520/GTJ10594J

22. Viggiani, G., Atkinson, J.H.: Interpretation of bender element tests. Geotechnique 149–154 (1995)

23. El Mohtar, C.S., Drnevich, V.P., Santagata, M., Bobet, A.: Combined resonant column and cyclic triaxial tests for measuring undrained shear modulus reduction of sand with plastic fines. Geotech. Test. J. **36**, 1–9 (2013). https://doi.org/10.1520/GTJ20120129

24. Kumar, S.S., Krishna, A.M., Dey, A.: Dynamic properties and liquefaction behaviour of cohesive soil in northeast India under staged cyclic loading. J. Rock Mech. Geotech. Eng. 1–10 (2018). https://doi.org/10.1016/j.jrmge.2018.04.004

25. Drnevich, V.P., Hardin, B.O., Shippy, D.J.: Modulus and damping of soils by the resonant column method. Dyn. Geotech. Test. Am. Soc. Test. Mater. Spec. Tech. Publ. **654**(654), 91–125 (1978)

26. Peacock, W., Seed, H.B.: Sand liquefaction under cyclic loading simple shear conditions. J. Soil Mech. Found. Div. **94**, 689–708 (1968)
27. Ishihara, K., Li, S.: Liquefaction of saturated sand in triaxial torsion shear test. Soils Found. **12**, 19–39 (1972)
28. Kokusho, T.: Cyclic triaxial test of dynamic soil properties for wide strain range. Soils Found. **20**, 45–59 (1980)
29. Saran, S.: Soil Dynamics and Machine Foundations. Galhotia Publication, New Delhi, India (1999)
30. Kashyap, S.S., Krishna, A.M., Dey, A.: Analysis of active MASW test data for a convergent shear wave velocity profile. In: Lehane, A.-M.K. (ed.) Geotechnical and Geophysical Site Characterisation, Sydney, Australia, pp. 951–956 (2016)
31. Taipodia, J., Dey, A., Baglari, D.: Influence of data acquisition and signal preprocessing parameters on the resolution of dispersion image from active MASW survey. J. Geophys. Eng. **15**, 1310–1326 (2018). https://doi.org/10.1088/1742-2140/aaaf4c
32. Foti, S., Hollender, F., Garofalo, F., et al.: Guidelines for the good practice of surface wave analysis: a product of the InterPACIFIC project. Bull. Earthq. Eng. **16**, 2367–2420 (2018). https://doi.org/10.1007/s10518-017-0206-7
33. Stokoe, K.H., Woods, R.D.: In situ shear wave velocity by cross-hole method. J. Soil Mech. Found. Div. **98**, 443–460 (1972)
34. Garofalo, F., Foti, S., Hollender, F., et al.: InterPACIFIC project: comparison of invasive and non-invasive methods for seismic site characterization. Part I: Intra-comparison of surface wave methods. Soil Dyn. Earthq. Eng. **82**, 222–240 (2016). https://doi.org/10.1016/j.soildyn.2015.12.010
35. Garofalo, F., Foti, S., Hollender, F., et al.: InterPACIFIC project: comparison of invasive and non-invasive methods for seismic site characterization. Part II: Inter-comparison between surface-wave and borehole methods. Soil Dyn. Earthq. Eng. **82**, 241–254 (2016). https://doi.org/10.1016/j.soildyn.2015.12.009
36. Taipodia, J., Ram, B., Baglari, D., et al.: Geophysical investigations for identification of subsurface. In: Indian Geotechnical Conference. JNTU, Kakinada (2014)
37. Lawrence, F.J.: Propagation velocity of ultrasonic waves through sand (1963)
38. Shirley, D.J., Hampton, L.D., Shirley, D.J., Hampton, L.D.: Shear-wave measurements in laboratory sediments. J. Accoustical Soc. Am. **63**, 607–613 (1978). https://doi.org/10.1121/1.381760
39. Shirley, D.J.: An improved shear wave transducer. J. Accoustical Soc. Am. **63**, 163–1645 (1978). https://doi.org/10.1121/1.381866
40. Arulnathan, R., Boulanger, R.W., Riemer, M.: Analysis of bender element tests. Geotech. Test. J. **21**, 120–131 (1998)
41. Kumar, S.S., Krishna, A.M., Dey, A.: Evaluation of dynamic properties of sandy soil at high cyclic strains. Soil Dyn. Earthq. Eng. **99**, 157–167 (2017). https://doi.org/10.1016/j.soildyn.2017.05.016
42. Iida, K.: The velocity of elastic waves in sand. Bull. Earthq. Res. Inst. **16**, 131–145 (1938)
43. Hardin, B.O.: Suggested Methods of Test for Shear Modulus and Damping of Soils by the Resonant Column, pp. 516–529 (1970)
44. Selig, E., Chung, R., Yokel, F., Drnevich, V.: Evaluation of dynamic properties of sands by resonant column testing. Geotech. Test. J. **7**, 60 (1984). https://doi.org/10.1520/GTJ10594J
45. ASTM D4015: Standard Test Methods for Modulus and Damping of Soils by Resonant-Column, pp. 1–22 (2014). https://doi.org/10.1520/d4015-07.1
46. Hall, J.R., Richart Jr., F.: Dissipation of elastic wave energy in granular soils. J. Soil Mech. Found. Div. **89**, 27–56 (1963)
47. Woods, R.D.: Measurement of dynamic soil properties: a state of the art. In: Proceedings of American Society of Civil Engineers Special Conference on Earthquake Engineering and Soil Dynamics, Pasadena, pp. 91–180 (1978)
48. Hardin, B.O., Music, J.: Apparatus for vibration of soil specimens during the triaxial test. ASTM STP **392**, 55–74 (1965)

49. Dammala, P.K., Kumar, S.S., Krishna, A.M., Bhattacharya, S.: Dynamic soil properties and liquefaction potential of northeast Indian soil for effective stress analysis. Bull. Earthq. Eng. (under review)
50. Sitharam, T., Govindaraju, L., Sridharan, A.: Dynamic properties and liquefaction potential of soils. Curr. Sci. 87:1370–1378 (2004)
51. Lombardi, D., Bhattacharya, S., Hyodo, M., Kaneko, T.: Undrained behaviour of two silica sands and practical implications for modelling SSI in liquefiable soils. Soil Dyn. Earthq. Eng. **66**, 293–304 (2014). https://doi.org/10.1016/j.soildyn.2014.07.010
52. Kumar, S., Krishna, A., Dey, A.: High strain dynamic properties of perfectly dry and saturated cohesionless soil. Indian Geotech. J. 1–9 (2017). https://doi.org/10.1007/s40098-017-0255-5
53. Kumar, S.S., Dey, A., Krishna, A.M.: Response of saturated cohesionless soil subjected to irregular seismic excitations. Nat. Hazards **93**, 509–529 (2018). https://doi.org/10.1007/s11069-018-3312-1
54. ASTM D3999: Standard test methods for the determination of the modulus and damping properties of soils using the cyclic triaxial apparatus. Am. Soc. Test. Mater. **91**, 1–16 (2003). https://doi.org/10.1520/d3999-11e01.1.6
55. ASTM D5311: Standard test method for load controlled cyclic triaxial strength of soil. Astm D5311 **92**, 1–11 (1996). https://doi.org/10.1520/d5311
56. Kjellman, W.: Testing the shear strength of clay in Sweden. Geotechnique **2**, 225–232 (1951)
57. Bjerrum, L., Landva, A.: Direct simple shear tests on a Norwegian quick clay. Geotechnique **16**, 1–20 (1966)
58. Lanzo, G., Vucetic, M., Doroudian, M.: Reduction of shear modulus at small strains in simple shear. J. Geotech. Geoenviron. Eng. **123**, 1035–1042 (1997). https://doi.org/10.1061/(asce)1090-0241(1997)123:11(1035)
59. Dammala, P.K., Adapa, M.K., Bhattacharya, S., Aingaran, S.: Cyclic response of cohesionless soil using cyclic simple shear testing. In: 6th International Conference on Recent Advances in Geotechnical Earthquake Engineering, ICRAGEE, pp. 1–10 (2016)
60. Seed, H.B., Idriss, I.M.: Soil moduli and damping factors for dynamic response analysis (1970)
61. Darendeli, M.: Development of a New Family of Normalized Modulus Reduction and Material Damping. University of Texas (2001)
62. Kumar, S.S., Adapa, M.K., Dey, A.: Importance of site-specific dynamic soil properties for seismic ground response studies. Int. J. Geotech. Earthq. Eng. (2018) (In press)
63. Bai, L.: Preloading Effects on Dynamic Sand Behavior by Resonant Column Tests. Technischen Universität, Berlin (2011)
64. Hardin, B.O.: The nature of stress-strain behavior of soils. In: Earthquake Engineering and Soil Dynamics. ASCE, Pasadena, CA, pp. 3–90 (1978)
65. Chattaraj, R., Sengupta, A.: Liquefaction potential and strain dependent dynamic properties of Kasai River sand. Soil Dyn. Earthq. Eng. **90**, 467–475 (2016). https://doi.org/10.1016/j.soildyn.2016.07.023
66. Saxena, S.K., Reddy, K.R.: Dynamic moduli and damping ratios for Monterey No.0 sand by resonant column tests. Soils Found. **29**, 37–51 (1989). https://doi.org/10.3208/sandf1972.29.2_37
67. Hardin, B.O., Drnevich, V.P.: Shear modulus and damping in soils: design equations and curves. J. Soil Mech. Found. Div. **SM7**, 667–692 (1972)
68. Ishibashi, I., Zhang, X.: Unified dynamic shear moduli and damping ratios of sand and clay. Soils Found. Jpn. Soc. Soil Mech. Found. Eng. **33**, 182–191 (1993). https://doi.org/10.1248/cpb.37.3229
69. Zhang, J., Andrus, R.D., Juang, C.H.: Normalized shear modulus and material damping ratio relationships. J. Geotech. Geoenviron. Eng. **131**, 453–464 (2005). https://doi.org/10.1061/(asce)1090-0241(2005)131:4(453)
70. Vardanega, P.J., Ph, D., Asce, M., et al.: Stiffness of clays and silts: normalizing shear modulus and shear strain. J. Geotech. Geoenviron. Eng. **9**, 1575–1589 (2013). https://doi.org/10.1061/(asce)gt.1943-5606.0000887

71. Matasovic, N., Vucetic, M.: Cyclic characterization of liquefiable sands. J. Geotech. Geoenviron. Eng. **119**, 1805–1822 (1994)
72. Hashash, Y.M., Dashti, S., Romero, M.I., et al.: Evaluation of 1-D seismic site response modeling of sand using centrifuge experiments. Soil Dyn. Earthq. Eng. **78**, 19–31 (2015)
73. Dobry, R., Pierce, W., Dyvik, R., et al.: Pore Pressure Model for Cyclic Straining of Sand. Troy, NY (1985)
74. Martin, G., Finn, W., Seed, H.: Fundamentals of liquefaction under cyclic loading. J. Geotech. Div. **101**, 423–438 (1975)
75. Byrne, P.: A cyclic shear-volume coupling and pore-pressure model for sand. In: Second International Conference on Recent Advances in Geotechnical Earthquake Engineering and Soil Dynamics, St. Louis, Missouri, pp. 47–55 (1991)
76. Hashash, Y.M.A., Musgrouve, M.I., Harmon, J.A., et al.: DEEPSOIL 6.1, User Manual (2016)
77. Vucetic, M., Dobry, R.: Cyclic triaxial strain-controlled testing of liquefiable sands. In: Advanced Triaxial Testing of Soil and Rock, pp. 475–485 (1988). https://doi.org/10.1520/stp29093s
78. Kirar, B., Maheshwari, B.K.: Dynamic properties of soils at large strains in Roorkee region using field and laboratory tests. Indian Geotech. J. **48**, 125–141 (2017). https://doi.org/10.1007/s40098-017-0258-2
79. Maheshwari, B.K., Kirar, B.: Dynamic properties of soils at low strains in Roorkee region using resonant column tests. Int. J. Geotech. Eng. **6362**, 1–12 (2017). https://doi.org/10.1080/19386362.2017.1365474
80. Dutta, T.T., Saride, S.: Influence of shear strain on the Poisson's ratio of clean sands. Geotech. Geol. Eng. **34**, 1359–1373 (2016). https://doi.org/10.1007/s10706-016-0047-1
81. Park, D., Hashash, Y.M.A.: Rate-dependent soil behavior in seismic site response analysis. Can. Geotech. J. **45**, 454–469 (2008). https://doi.org/10.1139/T07-090
82. Hashash, Y.M., Groholski, D.R.: Recent advances in non-linear site response analysis. In: Fifth International Conference on Recent Advances in Geotechnical Earthquake Engineering and Soil Dynamics Symposium, Honor Profr IM Idriss, vol. 29, pp. 1–22 (2010). https://doi.org/10.1016/j.soildyn.2008.12.004
83. Basu, D., Dey, A., Kumar, S.S.: One-dimensional effective stress non-Masing nonlinear ground response analysis of IIT Guwahati. Int. J. Geotech. Earthq. Eng. **8**, 1–27 (2017)
84. Kumar, S.S., Krishna, A.M.: Importance of site-specific dynamic soil properties for seismic ground response studies. Importance of site-specific dynamic soil properties for seismic ground response studies. Int. J. Geotech. Earthq. Eng. **9**, 1–21 (2018). https://doi.org/10.4018/IJGEE.2018010105
85. IS:1893: Criteria for earthquake resistant design of structures. Indian Stand. 1–44 (2002)
86. Ajom, B.E., Bhattacharjee, A.: Seismic re-qualification of Caisson supported Dhansiri River Bridge. In: Tunneling in Soft Ground, Ground Conditioning and Modification Techniques, pp 187–203 (2019)
87. Raghu Kanth, S.T.G., Sreelatha, S., Dash, S.K.: Ground motion estimation at Guwahati city for an Mw 8.1 earthquake in the Shillong plateau. Tectonophysics **448**, 98–114 (2008). https://doi.org/10.1016/j.tecto.2007.11.028
88. Kumar, A., Harinarayan, N.H., Baro, O.: High amplification factor for low amplitude ground motion: assessment for Delhi. Disaster Adv. **8**, 1–11 (2015)
89. Romero, S.M., Rix, G.: Ground Motion Amplification of Soils in the Upper Mississippi Embayment. MAE Center CD Release 05-01 (2005)